

THERMAL RESPONSE DURING COLD WATER REINJECTION IN NATURALLY FRACTURED GEOTHERMAL RESERVOIRS

Ascencio, F. (1); Rivera, J. (2) and Samaniego, F. (2)

(1) PEMEX EXPLORACION AND PRODUCCIÓN AND UNIVERSIDAD DE MICHOACÁN
(2) PEMEX EXPLORACION AND PRODUCCIÓN AND UNIVERSIDAD DE MÉXICO

Key Word: geothermal reservoir, underground fluid injection, naturally fractured systems.

ABSTRACT

Results are presented for a theoretical study of the heat transfer processes involved when separated cold water is reinjected into naturally fractured hot geothermal reservoir rock. This study considers the case when cold water is injected into a hot system initially placed at a given uniform temperature. The fractured system is modeled as two interconnected homogeneous systems, one for the matrix and the other one for the fractures. Heat and mass balances are established for the interconnected system when the cold injected fluid travels through the fracture system in close contact with a hot matrix system modeled as spheres, which act as a uniformly distributed heat source term in the fractured system. Solutions to this problem are presented for two cases: one in which instantaneous thermal equilibrium takes place between the injected cold fluid and the host rock, and the second one considers a nonthermal equilibrium situation for which solutions are derived for the cases when heat transfer occur under pseudo-steady state and transient conditions; solutions for these cases are compared. Solutions presented also consider heat interchange with underlying impermeable formation. Type-curve are presented which show the thermal front rate of advance with dimensionless injection time; also a sensitivity analysis was performed on the effect of several factors on the thermal front rate of advance, such as the intensity of rock-fracture interaction, ratio of thermal energy contained within the fractures to total system thermal energy, porosity, as well as Peclet and Biot numbers.

1. INTRODUCTION

Commercial exploitation of liquid dominated geothermal resources faces the problem of disposing in an environmentally safe way of large volumes of separated highly saline brine. This relatively cool brine is obtained as a by-product from the separation process to obtain the steam used to feed the turbines at the electrical power station. Separated fluids include non-condensable gases, mainly H_2S and CO_2 , as well as substances such as silicates and toxic compounds such as arsenic, boron and mercury, all of them concentrate in the liquid phase. Due to environmental regulations, this highly saline separated brine cannot be discarded of in surface without prohibitively expensive chemical treatments. To solve this problem, underground fluid injection of separated fluids for disposal purposes is usually carried out in geothermal fields.

It should be mentioned that when underground brine injection is carried out within the reservoir itself, it can have other

objectives than fluid disposal (Horne [1982a, 1982b, 1985], Schroeder et al [1980], Pruess and Bodvarsson [1984]):

- To provide additional pressure support in order to reduce the geothermal reservoir natural pressure decline due to fluid withdrawal.
- To improve total heat recovered from the resource through a secondary "heat mining" process from hot reservoir rock when contacted by cooler injected fluids, which otherwise would remain unrecovered in the resource.
- To reduce ground subsidence resulting from fluid extraction.

It should be mentioned that in spite of the positive aspects associated with underground fluid injection mentioned above, extreme care should be taken when such injection is to be performed into naturally fractured systems. In these system injected cool fluids could rapidly travel through open, communicated fracture rock networks, which usually connect injection and producing wells, establishing "short-circuits" for fluid circulation. When this "short-circuiting" occurs, injected cooler fluids will not have sufficient residence time in the reservoir to capture enough heat from surrounding hotter rock, resulting in undesirable fluid enthalpy decrease at producing wells. Since most geothermal reservoir are located in highly fractured igneous rocks, there have been several field experiences where detrimental effects due to cold fluid injection have been experienced (Horne [1982a, 1982b, 1985], Bodvarsson and Tsang [1982], Bodvarsson and Stefansson [1989], Gringarten et al [1975], Gringarten and Sauty [1975]).

When a relatively cold separated geothermal brine is injected in the hot reservoir, two distinct displacement fronts begin to develop and grow up around the injection well. The first front, known as the "chemical front", actually develops in the vicinity of the displacement front between the reservoir and the injected fluids. The second front, called the "thermal front"; whose temperature is lower than that corresponding to reservoir fluids, travels some distance behind the former. The chemical front has a temperature close to that of the reservoir fluid, and can be identified from differences in concentrations of chemical species present injected and reservoir fluids, respectively.

The mathematical model described in this paper presents solutions that allow the estimation of the distance that separates the chemical and thermal fronts within the reservoir at a given time, so that once the presence of the former is detected at producing wells from chemical analysis of produced fluids, an estimation of the location of the thermal front could be performed.

2. MATHEMATICAL MODEL

The idealized model for the physical situation under consideration in this study is illustrated in Fig. 1 for a linear

coordinate system (x, y, z), which can easily be extended to a cylindrical coordinate system (r, θ, z). Physical limits for this model are:

Permeable fractured stratum:

$$-\infty < x, y, < \infty; -H < z < 0$$

Upper impermeable stratum:

$$-\infty < x, y < \infty; 0 < z < \infty;$$

Lower impermeable stratum:

$$-\infty < x, y < \infty; -\infty < z < -H.$$

It should be mentioned that when dealing with the heat transfer phenomena for non-isothermal fluid flow through a permeable medium, consideration should be given as to whether such flow is taken place through a granular porous medium, or through a fractured system. For a given flow time, when fluid flow under non-isothermal conditions through a granular porous medium, there is a greater chance for thermal equilibrium to be rapidly reached between fluid and surrounding rock, since flow velocities are usually slow (except in vicinities of the injection well), and the grains surface area is large. On the other hand, if fluid is flowing through fractures, fluid velocities can be very fast, and the surface area available for heat transfer is smaller than that corresponding to a granular media, so that it will require fluid contact times with hot rock to attain thermal equilibrium much larger than those typical for a granular media.

2.1 SOLUTION CONSIDERING HEAT TRANSFER TO/FROM THE PERMEABLE STRATUM TO THE UPPER AND LOWER CONFINING STRATA

As discussed above, since some time is required for fluid flow through a naturally fractured stratum, for thermal equilibrium to be reached between the injected fluid and surrounding hot reservoir rock, independent energy conservation equations should be written for fluid and the rock matrix, coupled by means of a term representing the heat transfer rate interchanged between fluid and the rock. Assuming that fluid flow through the permeable fractured stratum is taking place under purely radial conditions, and that the horizontal conductive heat transfer rate is negligible for the permeable stratum and the confining strata, a dimensionless mathematical formulation for the heat transfer problem under consideration can be written as follows:

$$\frac{\partial T_{Ds}}{\partial t_D} = \frac{1}{a^2} \frac{\partial^2 T_{Ds}}{\partial z_D^2} \quad \begin{cases} 0 < z_D < \infty, \\ t_D > 0. \end{cases} \quad (1)$$

$$z_D = 0: \omega_f \frac{\partial T_{Df}}{\partial t_D} = \phi B_i (T_{Ds} - T_{Df}) - 2Pe \frac{\partial T_{Df}}{\partial \chi} -$$

$$\int_D^{t_D} \frac{\partial T_{Df}(\tau)}{\partial \tau} q_{Df}(t_D - \tau) d\tau \quad \begin{cases} 0 < \chi < \infty, \\ t_D > 0. \end{cases} \quad (2)$$

$$z_D = 0: \omega_r \frac{\partial T_{Ds}}{\partial t_D} = \kappa_{Dr} \frac{\partial T_{Ds}}{\partial z_D} - \phi B_i (T_{Ds} - T_{Df}) +$$

$$\int_D^{t_D} \frac{\partial T_{Df}(\tau)}{\partial \tau} q_{Df}(t_D - \tau) d\tau \quad \begin{cases} 0 < \chi < \infty, \\ t_D > 0. \end{cases} \quad (3)$$

$$T_{Df} = T_{Dr} = T_{Ds} = 0 \quad \begin{cases} 0 < \chi, z_D < \infty, \\ t_D = 0. \end{cases} \quad (4)$$

$$T_{Df} = 1 \quad \begin{cases} x = z_D = 0, \\ t_D > 0. \end{cases} \quad (5)$$

$$T_{Ds} \rightarrow 0 \quad \begin{cases} 0 < \chi < \infty, \\ z_D \rightarrow \infty, \\ t_D > 0. \end{cases} \quad (6)$$

Definitions of dimensionless variables is given in the Appendix. A complete derivation of eqs. (1) through (6) can be found in al Ascencio [1996].

It should be mentioned that Lauwerier [1955] presented an analytical solution to calculate the temperature distribution in a permeable stratum when a hot fluid is injected into a horizontal, homogeneous porous stratum, saturated with a cold fluid. He considered only convective heat transfer in the permeable stratum with instantaneous thermal equilibrium between fluid and rock grains, as well as heat transfer towards confining strata. As it can be seen both heat transfer problem can be treated by means of similar mathematical formulations.

It is convenient to recognize that eqs. (1)-(6) correspond to both linear and radial formulations of the problem under consideration, depending upon the definition used for the variable χ , thus if $\chi = x_D$ the problem formulation

corresponds to the linear case, whereas if $\chi = \frac{1}{2} r_D^2$ the problem formulation is for a radial system.

Dimensionless fluid and rock temperature distributions, T_{Df} and T_{Ds} are obtained as:

$$T_{Df} = \frac{1}{s} \exp \left(- \left\{ \left(\frac{\omega_r + b/\sqrt{s} - \bar{q}_{Df}(s)}{\omega_r s + b\sqrt{s} + \phi B_i} \right) \phi B_i + \bar{q}_{Df}(s) + \omega_f \right\} s \frac{\chi}{2Pe} \right) \quad (7)$$

$$T_{Ds} = \frac{\phi B_i + s \bar{q}_{Df}(s)}{s \omega_r + b \sqrt{s} + \phi B_i} T_{Df} \quad (8)$$

Dimensionless heat flux transfer functions are given by:

$$\bar{q}_{Df}(s) = \frac{\omega_r}{(\omega_r/\lambda_D)s + 1} \quad (9)$$

$$\bar{q}_{D1}(s) = k_{Dr}(A_{HTbD}/\epsilon) \frac{f(s)}{s(1 + \frac{1}{B_i} f(s))} \quad (10)$$

The dimensionless heat flux transfer function given by eq. (9) corresponds to the case when the heat transferred between the rock and the fluid takes place under pseudo-steady state conditions; while eq. (10) corresponds to transient heat flow conditions between fluid and spherical matrix blocks. In these equations $f(s)$ is given as:

$$f(s) = \sqrt{s \omega_r / \kappa_{Dr}} \epsilon \coth(\sqrt{s \omega_r / \kappa_{Dr}} \epsilon) - 1 \quad (11)$$

It has been shown Ascencio [1996] that for spherical matrix blocks the following relationships hold:

$$\lambda_D = \frac{\pi^2}{\epsilon^2 / \kappa_{Ds}}, \quad l_D = \frac{3(1-\phi)}{\pi^2} \epsilon \quad (12)$$

Substituting eq. (12) into eqs. (10) and (11):

$$\bar{q}_{D1}(s) = \frac{3(1-\phi)}{\pi^2} \lambda_D \frac{f(s)}{s(1 + \frac{1}{B_i} f(s))} \quad (13)$$

$$f(s) = \pi \sqrt{s \omega_r / \lambda_D} \coth(\pi \sqrt{s \omega_r / \lambda_D}) - 1 \quad (14)$$

For times large enough, $s \rightarrow \infty$ and $q_{D1} \approx \omega_r$, substituting these conditions into eqs. (7) and (8), they can be written as:

$$T_D = T_{Df} = T_{Ds} = \frac{1}{s} \exp\left(\left(b/\sqrt{s} + 1\right)s \frac{\chi}{2Pe}\right) \quad (15)$$

The inverse Laplace's transformation of (15) can be expressed as:

$$T_D(\chi, t_D) = \operatorname{erfc} \frac{b \frac{\chi}{2Pe}}{2\sqrt{t_D - \frac{\chi}{2Pe}}} U(t_D - \frac{\chi}{2Pe}) \quad (16)$$

It should be mentioned that eq. (16) is analogous to the solution previously published by Lauwerier [1955]. However, when instantaneous, it is not possible to find an analytical expression for the Laplace's inverse transformation of eq. (7). Therefore, for these conditions, T_{Df} can be obtained from a numerical algorithm for Laplace's inverse transforms. For this purpose the Stehfest algorithm was used in this work.

3. EXPRESSIONS FOR THE THERMAL FRONT

The thermal front is defined as the geometric locus described by fluid particles flowing through the fracture network whose temperature, T_{TF} has been decreased by a given fraction of the temperature difference between the resident reservoir fluids and the injected fluid temperature.

$$T_{TF} = T_i + f(T_D - T_i) \quad (17)$$

For a symmetrical thermal front $f = 1/2$; however, experience has shown that actual thermal fronts are highly asymmetrical. Based upon field practical observations,

Pruess and Bodvarsson [1984], suggested to use a value of $f = 3/4$. Using this value, dimensionless thermal front can be expressed as:

$$T_{TF} = 1/4 \quad (18)$$

A type-curve was constructed taking into account eq. (18) for the thermal front, eq. (18) inverted numerically by means of the Stehfest algorithm to find the fluid temperature distribution flowing through the fractured stratum, as well as the heat flux transference function between rock and fluid, given by eq. (13).

Upon this type-curve, sensitivity was performed to find out the effect of the main dimensionless parameters associated with the heat transfer process upon the development of such thermal front. Transient and pseudo-steady heat transfer conditions between fluid and rock matrix were considered. To construct the type curve shown in Fig. 2, typical values of geothermal fractured systems were considered for evaluating several dimensionless parameters. Table 1 show values considered to this end.

3.1 DISCUSSION OF THE TYPE CURVE

As it can be seen from Fig. 2 four periods can be identified during the development and growth of the thermal front in a permeable fractured stratum.

1. *Early time period.* At early times both the chemical (or hydrodynamical) front, CF, and thermal front, TF, travel together for some time. During this period heat transferred from rock matrix has not yet started to develop the TF. Dimensionless distances traveled by the TF during this period for the linear and radial cases are, respectively:

$$x_{DTF} = 2Pe't_D/\omega_r \quad (19)$$

$$\chi_{TF} = 2Pe't_D/\omega_r \quad (20)$$

In terms of real variables these distances are:

$$x_{TF} = x_{CF} = (V/\phi)t \quad (21)$$

$$r_{TF} = r_{CF} = \sqrt{\frac{q_i t}{\phi \pi H}} \quad (22)$$

2. *Transition Period.* At intermediate dimensionless times a transition region develops. During this period heat is transferred from the matrix rock to the fluid traveling through the fractures producing a delay in the TF with respect to the CF, which shows as a departure of the TF curve from the early straight line. Duration of this period should be expected to be strongly dependent on heterogeneity of the fractured medium.

3. *Thermal Equilibrium Period.* At dimensionless times long enough, thermal equilibrium is finally reached in the heat transfer process, which shows in Fig. 2 as the TF curve gets further away from the CF curve and approaches and finally meets the instantaneous thermal equilibrium solution, ITE, and from there on follows it for some time interval. During this period any heat transferred to or from the upper and lower confining strata is negligible. Dimensionless distances traveled by the TF for the linear and radial cases are, respectively:

$$x_{DTF} = 2Pe't_D \quad (23)$$

$$\chi_{TF} = 2Pe t_D \quad (24)$$

In terms of real variables these distances are:

$$x_{TF} = \omega_f (V/\phi) t, \quad (25)$$

$$r_{TF} = \sqrt{\omega_f \frac{q_i t}{\phi \pi H}} \quad (26)$$

Late Time Period. At dimensionless times long enough for heat transferred from the confining strata to show up, the *TF* curve starts to depart from the *ITE* curve, bending to the right as time continues to proceed, as shown in the upper right hand side corner of Fig. 2.

Since location of the *CF* and the *TF* are given for any dimensionless time in Fig. 2, and as it can be observed from this figure, both fronts follow parallel log-log straight lines during the Thermal Equilibrium Period, then as shown by Ascencio and Rivera (1994), the distance between both fronts can be expressed for the linear and radial cases, respectively, as:

$$\delta_l = x_{CF} - x_{TF} = (1 - \omega_f) x_{CF} \quad (27)$$

$$\delta_r = r_{CF} - r_{TF} = (1 - \sqrt{\omega_f}) r_{CF} \quad (28)$$

From the analysis of variables involved in the construction of Fig. 2, it can be shown that ω_f has a direct effect on the duration of the transition period. The duration of the transition period, Δt_{tp} , can be calculated for the linear and radial cases from the following expression

$$\Delta t_{tp} = t_{TF} - t_{CF} = \left(\frac{1}{\omega_f} - 1 \right) t_{CF} \quad (29)$$

where t_{CF} and t_{TF} are arrival times for the chemical and thermal front, respectively.

From Fig. 2 it is apparent that the transition period starts earlier for transient heat flow conditions from the matrix to the fluid in the fractured medium and lasts longer than in the case when this heat is transferred under pseudo-steady state conditions. It can also be seen that transition from the Early Time Period towards the Thermal Equilibrium Period takes place in a smoother way for the transition heat flow condition than for the pseudo-steady state one. The end of the Thermal Equilibrium Period and the beginning of the Late Time Period is marked by the late time departure from the thermal equilibrium condition identify by the log-log straight line in Fig. 2, once heat transferred from confining strata starts to show up. Conditions to reach the Late Time Period are:

$$t_D \geq 0.1 \quad (30)$$

$$\frac{\chi}{2Pe} \geq 0.1 \quad (31)$$

4. EXAMPLE OF APPLICATION

To illustrate the application of the model presented in this paper, the following synthetic field example is presented: In a given geothermal underground injection project a cool separated brine is injected back in the hot naturally fractured

reservoir for a period of one year, at a constant volumetric flow rate of $0.03 \text{ m}^3/\text{s}$. Assuming a purely radial fluid flow pattern away from the injection well, and that the temperature difference between injected and reservoir resident fluids is of 50°C , and considering thicknesses of the permeable fractured stratum of 10 m , 100 m and 1000 m . Calculate the location from the injection well of the chemical and thermal fronts, considering:

- There is heat transferred from the confining strata to the permeable fractured stratum.
- Any heat transferred from the confining stratum to the hot fractured stratum is negligible.

Thermophysical properties for the fluid, the dry hot matrix rock, and the fluid saturated hot matrix rock are given in Table. 2.

4.1 Solution

Dimensionless, times t_D , are calculated for the three values of H (10 , 100 and 1000 m) by means of eq. (32) from Appendix, results are shown in the second column of Table 3.

Values for the ordinate $\frac{\chi}{2Pe}$ are then determined from the curve for the permeable fractured stratum in Fig. 2 corresponding to t_D values previously calculated. Table 3 shows $\frac{\chi}{2Pe}$ values in column 3.

The location of the thermal front can be calculated from eq. (26); meanwhile the location of the chemical (hydrodynamic) front can be determined from eq. (22). Results of these calculations are included in Table 3, in column 4 and 5, respectively. Values within squared brackets in column 5 correspond to the cases when there is no heat transferred from the confining strata to the permeable fractured stratum.

4.2 Additional Comments on the Synthetic Field Example

As it can be seen from an analysis of Table 3, the thickness of the permeable stratum is very important in the heat transfer problem considered, since holding all other parameters constant, 10 fold changes in its magnitude covered three flowing periods previously described in the type curve presented in this paper. Transition Period for $H = 1000 \text{ m}$, Thermal Equilibrium Period for $H = 100 \text{ m}$ and Late Time Period for $H = 10 \text{ m}$ in Table 3. It can be seen that the net effect of the heat transferred from the confining strata to the permeable fractured horizon, when present, is to slow down the rate of advance of the thermal front, compared to that observed when there is not such heat contribution, as it is apparent from the two values for r_{TF} calculated under both conditions. From Table 3 it can be seen that for the larger fractured stratum thickness considered in the example, $H = 1000 \text{ m}$, it is evident that from calculated values the thermal front has traveled further than predicted by the thermal equilibrium theory.

5. CONCLUSIONS

Based upon theoretical developments and results included in this paper the following conclusions can be drawn:

- A mathematical model has been presented to solve the heat transfer problem for non isothermal underground fluid injection through a naturally fractured stratum. Expressions were presented for calculation of temperature profiles for the fluid flowing through the fractured system, as well as for the rock matrix, both under instantaneous and non-instantaneous thermal equilibrium conditions. The model can consider rock/fluid heat transfer under either transient or pseudo-steady state conditions.
- A type-curve was presented to describe the development and growth of the chemical (or hydrodynamical) front and of the thermal front that are present when a relatively cool injected fluid displaces a hot resident geothermal fluid through a naturally fractured stratum. Rate of advance of the thermal front is characterized by four distinct flowing periods: 1. *Early Time Period*. 2. *Transition Period*. 3. *Thermal Equilibrium Period*. 4. *Late Time Period*.
- The main parameters affecting the temperature distribution within the permeable fractured stratum during a non-isothermal fluid injection are:

$$\omega_f, \lambda_D, Pe, H.$$

- Parameter λ_D determines the beginning of the transition period. It is an indication of the medium.
- The effect of heat transferred from impermeable confining strata towards the permeable fractured strata, when present, is to slow down the rate of advance of the thermal front, compared with its rate of advance under thermal equilibrium conditions, when such contribution is negligible.

REFERENCES

Ascencio, F. and Rivera, J. (1994). Heat transfer processes during low or high enthalpy fluid injection into naturally fractured reservoir". *Nineteenth annual workshop on Geothermal Reservoir Engineering*. Stanford U. 19:81-87. January 18-20, 1994.

Ascencio, F. (1996). Procesos de transferencia de calor en medios naturalmente fracturados. Tesis doctoral. Facultad de Ingeniería de la Universidad Nacional Autónoma de México.

Bodvarsson, G. S. and Stefansson, V. (1989). Some Theoretical and Field Aspects of Re-injection in Geothermal Reservoirs. *Water Resour. Res.*, 15(6), pp.1235-1248.

Bodvarsson, G.S. and Tsang, C.P. (1982). Injection and Thermal Breakthrough in Fractured Geothermal Reservoirs. *J. of Geophysical Research*, 87, p1031.

Gringarten, A.C. and Sauty, J.P. (1975). A Theoretical Study of Heat Extraction from Aquifers with Uniform Regional Flow. *J. Geophysical Research*. Vol. 80(5), pp. 4956-4962.

Gringarten, A.C., P.A. Witherspoon and Y. Onishi. (1975). Theory of Heat Extraction from Fractured Hot Dry Rock. *J. Geophys. Res.* Vol. 89(8), pp.1120-1124.

Horne, R.N. (1982). Effects of Water Injection Into Fractured Geothermal Reservoirs: A Summary of Experience Worldwide. *Geothermal Resources Council*, pp.47-63.

Horne, R.N. (1982). Geothermal Re-injection in Japan. *J. Pet. Tech.*, pp.495-503.

Horne, R.N. (1985). Reservoirs Engineering Aspects of Re-injection. *Geothermics*. Vol. 14(2), pp.449-457.

Lauwerier, H.A. (1955). The transport of heat in an oil layer caused by the injection of hot fluid. *Appl. Sci. Res.* Vol. 5, pp.145-150.

Pruess, K. and Bodvarsson, G.S. (1984). Thermal Effects of Re-injection in Geothermal Reservoir with Major Vertical Fractures. *J. Pet. Tech.*, Sept.

Schroeder, R.C., O'Sullivan, M.J. and Pruess, K. (1980). Re-injection Studies of Vapor Dominated Systems. Paper presented at the Italian-American Workshop, Oct.

NOMENCLATURE

Italic Letters:

A_{THb}	Effective heat transfer area unit of total volume, m
c	fluid heat capacity, $J/kg \ ^\circ C$
\hat{h}	convective heat transfer coefficient, $J/m^2 s \ ^\circ C$
h'	fracture thickness, m
H	permeable fractured stratum thickness, m
l	rock matrix block characteristic length, m
q_i	volumetric fluid injection rate, m^3/s
q^*	matrix-fracture heat flux interchange rate per unit of total volume, $J/m^3 s$
q_1	heat flux rate per unit temperature drop at a surface, $J/m^3 s \ ^\circ C$
r_b	rock matrix spherical block radius, m
s	Laplace's transformation parameter
T	temperature, $^\circ C$
v	microscopic velocity, m/s
V	macroscopic (Darcy's) velocity ($= \phi v$), m/s

Roman Letters:

B_i Biot number

Pe Peclet number

Greek letters:

α thermal diffusivity ($= k / \rho c$), m^2/s

α' fluid saturated rock thermal diffusivity, ($= A_{THb} / l$), m

$\bar{\alpha}$ fluid saturated rock thermal diffusivity, m^2/s

δ_i	defined by eq. (27), m
δ_r	defined by eq. (28), m
ΔT	temperature difference $T_o - T$, $^{\circ}C$
κ	thermal conductivity, $J/m s ^{\circ}C$
κ'	fluid saturated rock thermal conductivity, $J/m s ^{\circ}C$
λ	rock/fracture interaction coefficient ($= k_r A_{THb} / l$), J ,
ε	$= 2r' / H$
ρ	density, kg/m^3
ρc	fluid saturated rock heat capacity, $J/kg m^3$
ϕ	porosity
ω_f	rate of energy within fractures to total system energy
ω_r	rate of energy within rock matrix to total system energy
Subindexes:	
b	rock matrix block
CF	chemical (hydrodynamical) from
D	dimensionless
f	fluid (or fracture)
HTb	heat transferred per unit of total volume
i	injection
s	impermeable stratum
TF	thermal front
o	initial
1	unit temperature drop at rock/fluid interphase

APPENDIX

Dimensionless variables used in this paper are defined as follows.

Dimensionless time, t_D , is

$$t_D = \frac{4\kappa t}{\rho c H^2} = \frac{4\alpha t}{H^2} \quad (32)$$

where $\overline{\alpha}$ is the thermal diffusivity for the fully saturated medium.

Dimensionless temperature are:

$$T_D = \frac{T_o - T}{T_o - T_i} \quad (33)$$

Thus, for T_s , T_f , T_r and T_b :

$$T_{Ds} = \frac{T_o - T_s}{T_o - T_i}, \quad T_{Df} = \frac{T_o - T_f}{T_o - T_i}, \quad (34)$$

$$T_{Dr} = \frac{T_o - T_r}{T_o - T_i}, \quad T_{Db} = \frac{T_o - T_b}{T_o - T_i}$$

Spatial dimensionless parameters:

$$r_D = \frac{2r}{H}, \quad \chi = \frac{1}{2} r_D^2, \quad r'_D = \frac{2r'}{H}, \quad z_D = \frac{2z}{H}, \quad x_D = \frac{2x}{H}, \quad t_D = \frac{2l}{H} \quad (35)$$

$$A_{HTbD} = A_{HTb} \frac{H}{2}, \quad \lambda_D = k_{Dr} (A_{HTbD} / l_D) \quad (36)$$

ω_f and ω_r :

$$\omega_f = \frac{\rho c_f c_f}{\rho c}, \quad \omega_r = \frac{(1-\phi)\rho_r c_r}{\rho c} \quad (37)$$

Thermophysical dimensionless parameters;

$$\alpha^2 = \frac{\alpha_s}{\alpha}, \quad b = \frac{\kappa_{Ds}}{\alpha} = \sqrt{\rho_s c_s \kappa_s} / \sqrt{\rho c \kappa} \quad (38)$$

$$\kappa_D = \frac{\kappa}{\kappa} \quad (39)$$

Therefore, for fluid and media:

$$\kappa_{Df} = \frac{\kappa_f}{\kappa}, \quad k_{Dr} = \frac{\kappa_r}{\kappa}, \quad k_{Ds} = \frac{\kappa_s}{\kappa} \quad (40)$$

Biot and Peclet dimensionless groups:

$$B_i = \frac{\hat{h}H}{2\kappa}, \quad \hat{B}_i = \frac{\hat{h}H}{2\kappa_r} \quad (41)$$

$$Pe = \frac{\rho_f c_f q_i}{4\pi H \kappa} = \frac{\omega_f (q_i / \phi)}{4\pi H \alpha}, \quad Pe' = \frac{\rho_f c_f VH}{4\kappa} = \frac{\omega_f VH}{4\alpha} \quad (42)$$

Dimensionless heat flux:

$$q_D^* = \frac{H^2 q^*}{4k} \quad (43)$$

Table 1. References parameters

λ_D	100 000
ω_f	0.10
ϕ	0.1
ϕB_i	100
B_i	∞
b	1

Table 2. Characteristic geothermal reservoir parameters

Fluid	
Density, $\rho_f, \text{kg/m}^3$	1000
Specific heat, $c_f, \text{J/kgm}^3$	4200
Thermal conductivity, $k_f, \text{W/m } ^\circ\text{C}$,	1
Rock	
Porosity,	0.1
Density, $\rho_r, \text{kg/m}^3$	2700
Specific heat, $c_r, \text{J/kgm}^3$,	1000
Thermal conductivity, $k_r, \text{W/m } ^\circ\text{C}$,	2
Saturated Rock	
Specific heat, $\bar{\rho} \bar{c}, \text{J/kgm}^3$	2.8×10^6
Thermal conductivity, $\bar{k}_r, \text{W/m } ^\circ\text{C}$,	1.9
Other s	
$b (= \sqrt{\rho_s c_s k_s} / \sqrt{\bar{\rho} \bar{c} \bar{k}}),$	=1
$\omega_f (= \phi_f \rho c_f / \bar{\rho} \bar{c}),$.15
B_i	∞
λ_D	100 000

Table 3. Summary of calculations for example

$H(m)$	t_D	$\frac{\chi}{2Pe}$	$r_{TF}(m)$	$r_{CF} (m)$
10	8.4×10^{-1}	6.5×10^{-1}	185(211)	542
100	8.4×10^{-3}	8.4×10^{-3}	67(67)	173
1000	8.4×10^{-5}	1.2×10^{-4}	25(21)	55

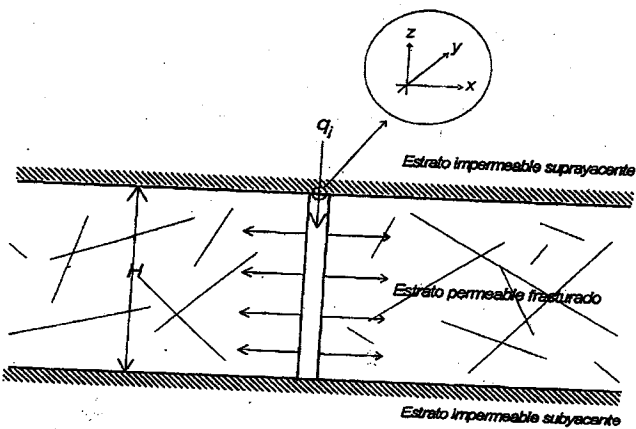


Fig. 1 Idealized model for the underground fluid injection problem under consideration.

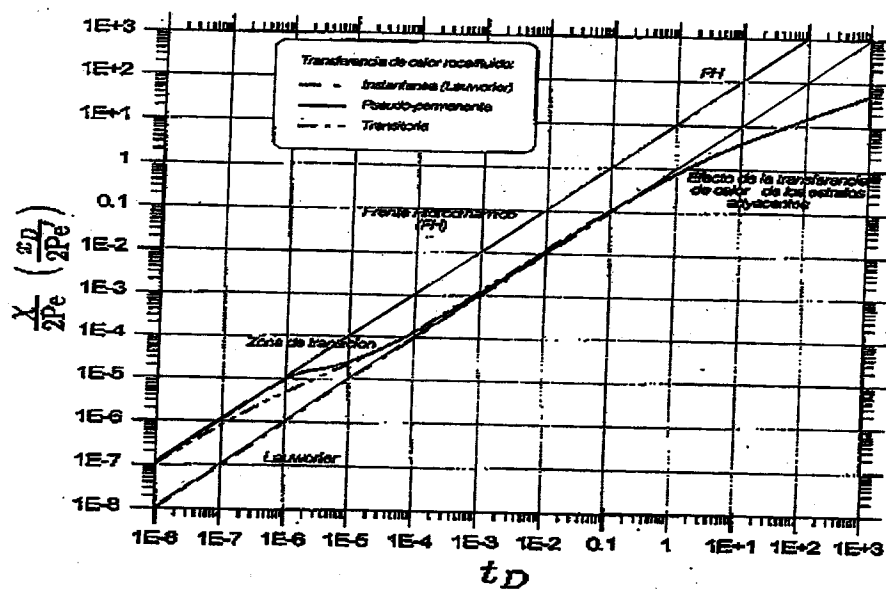


Fig. 2 Development and growth of the thermal front for non-isothermal fluid injection in a naturally fractured system.